Dynamic buckling of composite mast panels of sail ships

Marco Gaiotti, Stefano Ghelardi, Cesare Mario Rizzo
Università di Genova, Genova, Italy

ABSTRACT: Composite materials are becoming more and more popular, even for large ship and offshore structures. They offer lightweight and adaptable strength and stiffness properties. In case of slender structures, where buckling is the governing limit state, such features are valuable and allow designing high performance assemblies like racing crafts as well as very large sail ships. The case of composite masts of sail ships is rather interesting as, on the one hand, relatively large, stiff but light structures are needed and, on the other hand, their reliability is crucial for ship safety. Hence, complete understanding of structural behaviour is essential to avoid too large safety factors. Indeed, such case is also the paradigm of the dynamic buckling behaviour of slender columns structures, pointing out differences between the widely used quasi-static design approach and the more realistic time domain simulations. An earlier work studied the dynamic buckling behaviour of a metallic mast. Now, the study has been extended to the much more complex case of composite masts, showing some variations due to anisotropic material properties and specific weight values different by an order of magnitude. Comprehensive description of the dynamic buckling of a typical composite mast panel is outlined in this paper and compared to results from a previous investigation on aluminium alloy mast.

1 INTRODUCTION

This paper deals with a mast panel of a large sail ships. The design of these charming slender structures is theoretically and computationally demanding. However, it should be admitted that their design is still largely based on empiricism, even if in the last years rule requirements are more and more introducing state-of-the-art structural analysis methods involving numerical analyses besides scantling check approximated formulae. Really, only design of racing boats and of large sail ships are in general deemed worth of advanced numerical analyses and simulations involving computational fluid dynamics (CFD), finite element analyses (FEAs) and, eventually, complete fluid structure interaction (FSI) calculations like e.g. those carried out by Trimarchi and Rizzo (2009). Publications on this topic mostly deal with the aerodynamics of sails (Viola *et al.* 2014) and more recently investigated the FSI like in Sacher *et al.* (2015). Shenoi *et al*. (2009) had previously summarized the state of the art about structural analyses, reporting a widespread literature review showing qualitative descriptions and rules of thumb: indeed, no innovative approaches for the scantling design of mast and rigging has been proposed since many decades. The behaviour of the rigging system under wind gusts and the dynamic forces on the mast due to vessel motions in rough sea are still quite hard to predict. Similarly, the pre-tensioning loads led by dock tuning and their variations over time induced by mast and sail trimming are largely unknown along with several other parameters, as noted in Rizzo *et al.* (2009). Some evaluations on the rig's tuning accounting for ship motions have been reported by Fossati and Muggiasca (2011), who carried out a study in wind tunnel environment and by Augier et al. (2013), who exploited numerical FSI simulations. However, while highlighting the dynamic aspects of sail systems loading, both works focused on the influence of the ship motions and rig's tuning on yacht performances, and they were limited mainly to the aerodynamic aspects of the problem. A study mainly dedicated to structural aspects was published by Menotti et al. (2010). The authors investigated the reasons of the dismasting of the Volvo 70 Groupama 4 team sailboat through an FSI approach, coupling a potential flow code with FEAs. Results showed the loss of different structural elements of the rigging system led to the mast failure. In a recent publication, Lepidi *et al.* (2015) proposed a simplified mono-dimensional analytic model developed for preliminary design to assess the response of the rig under periodic pitching motions. Model's results were validated with nonlinear FEAs. Another important aspect in rig scantling is represented by fabrication defects affecting the mast structural response, as reported by Lorenzetti *et al.* (2017). In this works, the authors set up a FEM beam model able to take into account local defect affecting the local and global stability of the mast.

Rizzo and Boote (2010) identified the elastic buckling as the governing limit state for mast and rigging slender structures, showing an overview of their modern scantling design procedures. However, yielding and other nonlinear collapse mechanisms affecting ultimate strength should be investigated as well, considering that weight reduction is of paramount importance due to its significant effect on ship's stability and sea-keeping behaviour. Moreover, they noted that

procedures for rig design found in open literature as well as in some scantling rules (e.g. the Nordic Boat Standard, the Bureau Veritas rules and the Det Norske Veritas rules) are traditionally based on the well-established Skene's analytical method (Skene, 1938), which considers a quasi-static equilibrium between inclining and righting moments, in order to estimate acting forces on mast and rigging. Global mast buckling is the only limit state to be checked, as long as other failure mechanisms are implicitly prevented by safety factors. More refined scantling methods, taking advantage of modern computational facilities, were outlined as well by Rizzo and Boote (2010), showing that other limit states can be well assessed even by FEAs using only truss and beam elements. Sub-modelling technique can be applied to assess local behaviour of parts of the sail system like a mast panel.

FEAs are more regularly used by rigs designers and, recently, required by rules of classification societies dealing with sail systems approval. Actually, maritime administrations, like e.g. those of the Red Ensign group, currently require design approval of mast and rigging of large sail yachts. Some classification societies issued relevant rules. DNVGL rules, originating from those of the Germanisher Lloyd before the merging with the Det Norske Veritas, provide a detailed description of structural analyses to be carried out, addressing composite materials as well.

This work represents an extension of the study presented by Gaiotti and Rizzo (2014), where the dynamic behaviour of an aluminium mast of a large sail ship under dynamic conditions was investigated. There, the dynamic buckling of the lowest panel of a very large mast was considered and several numerical analyses were carried out to assess whether dynamic phenomena affect the structural behaviour. It was concluded that wave-induced loads on a large sail ship are varying in time in a frequency range, which is sensitive for the buckling behaviour of this slender structures. Reference is made to this earlier work where a general introduction to the subject is also given. Hereunder, the focus is on a composite mast and its dynamic buckling behavior, showing differences with respect to the metallic structure. In order to be consistent with the previous work and to allow comparison of results, the very same loading and boundary conditions were maintained while a different structure has been assessed as described in the following section. Eventually, a proper deep investigation on the materials used for building such structures (i.e. aluminium alloys, carbon fibres) should be carried out in order to assess for possible different limit states, depending on the employed material.

2 TEST CASE

The test case considered in this paper refers to an actual Carbon Fibers Reinforced Plastic (CFRP) mast typically employed in sailing boat industry.

The cross section of the mast is reported in Figure 1. The mast cross section has no internal stiffening members and it is built in two parts, obtained by moulding. The parts are later joined by overlapping the laminate skins. This overlapping also constitutes a local reinforcement in way of the mast sides. The total thickness of the shell laminate is 4.0 mm everywhere, except in way of the overlapping skins where it is 8.0 mm. The mid-thickness of the shell structure is sketched in Figure 2.

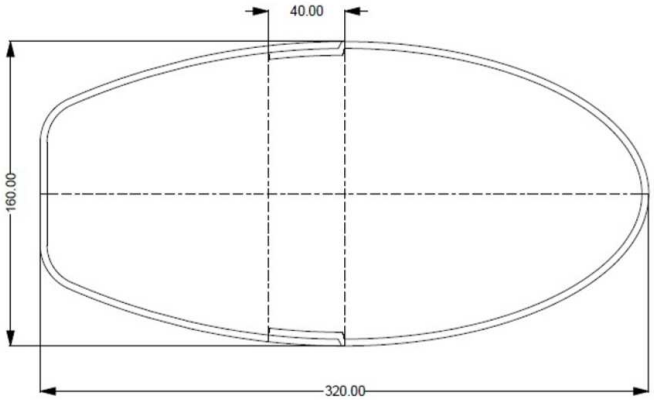

Figure 1. Mast cross section [mm]

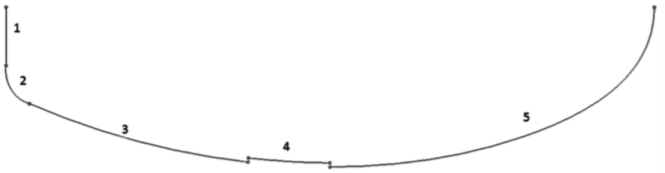

Figure 2. Half section sketch using spline curves

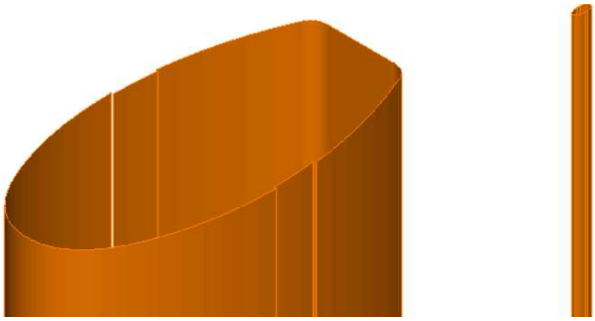

Figure 3. Geometry of the panel (top detail on left)

The current analysis aims at investigating a column-like structure, to represent the lowest panel of a typical mast structure. The column is 10.0 m high in the numerical investigation, as in Gaiotti and Rizzo (2014), representing the average distance from the mast step to the lowest spreader in large sailing yachts. The geometry has been obtained by extruding the cross section (**Errore. L'origine riferimento non è stata trovata.**). Plies employed in the stacking sequence are 0°/90°, ∓ 45° and uni-directional standard carbon fibres fabrics. Plies' characteristics are reported in Table 1. Biaxial layers' nominal thickness is 0.6 mm, whilst uni-directional layers are 0.4 mm thick.

An orthotropic plastic material model has been adopted for the plies, assuming a quasi-null plastic re-

sidual deformation, in order to simulate a brittle collapse behaviour typical of fibre-reinforced plastics. Tsai-Hill failure criterion has been considered to define the limit of the elastic behaviour of the material. For a plane stress condition, assumed in the present numerical simulation as reasonable simplification due to the limited thickness of the composite laminate, the criterion is reported in Equation 1:

$$\frac{\sigma_{11}^2}{R_{11}^2} - \frac{\sigma_{11}\sigma_{22}}{R_{11}^2} + \frac{\sigma_{22}^2}{R_{22}^2} + \frac{\tau_{12}^2}{R_{12}^2} \leq 1 \qquad (1)$$

where σ_{11} and σ_{22} are the axial and normal stress components, referred to fibre direction, τ_{12} is the in-plane shear stress, whilst corresponding R values are the relevant failure stresses. It is worth remembering that Tsai-Hill criterion cannot account for both tension and compression at the same time, but the failure stresses have to be considered according to the actual stress of the laminate, especially when the material presents a different behaviour in tension and in compression, likewise in composites.

Table 1. Plies' mechanical properties, being
0/90 : Stnd. 0/90 CF Fabric
±45 : Stnd. ±45 CF Fabric
UDE : Stnd. UDE

	Units	0/90	±45	UDE
Young Modulus 0°	[GPa]	70	17	135
Young Modulus 90°	[GPa]	70	17	10
In-Plane Shear Modulus	[GPa]	5	33	5
Major Poisson Ratio	[-]	0.10	0.77	0.30
Ultimate Tensile Strength 0°	[MPa]	600	110	1500
Ultimate Compressive Strength 0°	[MPa]	570	110	1200
Ultimate Tensile Strength 90°	[MPa]	600	110	50
Ultimate Compressive Strength 90°	[MPa]	570	110	250
Ultimate In-Plane Shear Stress	[MPa]	90	260	70
Ultimate Tensile Strain 0°	%	0.85	-	1.05
Ultimate Compressive Strain 0°	%	0.80	-	0.35
Ultimate Tensile Strain 90°	%	0.85	-	0.5
Ultimate Compressive Strain 90°	%	0.80	-	1.5
Ultimate In-Plane Shear Strain	%	1.80	-	2.4
Density	kg/m3	1600	1600	1600

3 NUMERICAL MODEL

A finite shell elements model has been built in the ADINA (2016) software environment to simulate the mast geometry under investigation. Twenty-four thousand Mixed Interpolated Tensorial Components 4-nodes (MITC4) shell elements have been applied to discretize the whole mode, see Chapelle and Bathe (2011). Large displacements due to elastic instability up to structural failure and material non-linearities in the post-elastic range, describing material failure, justify the adoption of a non-linear element.
Panel's own weight is computed by a consistent mass matrix, while the weight of the upper part of the mast (not modelled) is estimated to be 5000 kg, considering typical masts of this size. It is worth noting that comparative design analyses on sail systems showed that carbon mast weight is of the same order of magnitude of light alloy one. Such mass is applied as a concentrated mass on the centre of gravity of the top cross section and connected to the tube shell elements

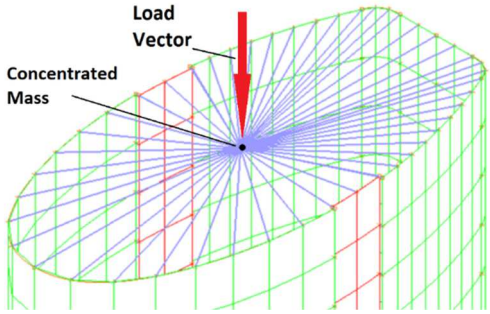

by means of rigid links, see Figure 4.
Figure 4. Finite shell elements model top side, rigid links, load vector and concentrated mass

This assumption represents a simplification, since rotational inertial effects are lost and a purely diagonal mass matrix is adopted. At this stage of the research on the dynamic buckling, the rotational inertia of the top part of the mast structure, also due to mast prebend, is thus neglected.

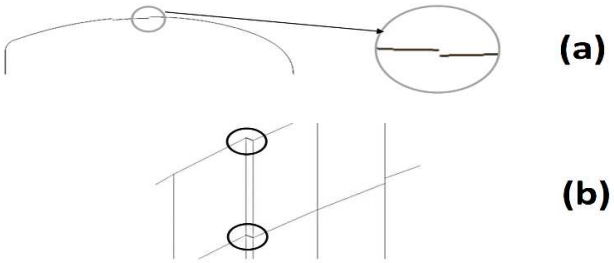

Figure 5. (a) Mast shell mid plane. (b) Rigid links connecting shell elements

The mast is fully clamped at its bottom while the shape of the cross section is fixed by a rigid link set in the upper end, where load is applied. Since mast's geometry has been simplified by modelling shell elements mid surfaces, a gap was generated between the flanges zones and the rest of the shell (Figure 5 (a)). Therefore, panels have been connected through rigid links as reported in Figure 5 (b)

4 STATIC COLLAPSE ANALYSIS

A preliminary static collapse analysis has been performed to investigate the collapse mechanism and to define the post-buckling response. Even if very large displacements are found, a wide part of the post buckling phase is still within the material elastic range. The computation is carried out through a FE Eigenvalue linearized buckling analysis, whose results return the buckling mode shapes to be imported as initial imperfection for a non-linear progressive collapse model as suggested e.g. by Bathe (1996).

As regards the Eigenvalue calculation, in the present case, a load of 100 kN was applied resulting in a load factor, i.e. a scaling factor identifying the buckling load, equal to 1.516 for the first buckling mode. Therefore, in this case, the buckling load resulted to be 151.6 kN. It should be noted that the load was applied as a force in the same node where the concentrated mass was imposed and spread on the mast surface by means of rigid links (Figure 4).
Afterwards, a full non-linear collapse analysis has been carried out. The first buckled mode shape has been set as initial imperfection with a maximum amplitude of Y=0.1 mm transverse displacement in the Y direction, in way of the node showing the maximum lateral displacement in the linearized analysis, i.e. roughly at mid span.
Raftoyiannis and Spyrakos (1997), among the others, described the impact of the initial imperfection on the post-buckling transition. Indeed, the transition becomes smoother and the critical load threshold can hardly be identified, while increasing the imperfection amplitude. Hence, a rather small value of the initial imperfection was selected, certainly well lower than actual geometrical imperfections. The computation has been carried out in displacement-controlled regime, meaning that a compressive displacement in Z direction has been applied linearly increasing from 0.0 to 100.0 mm. The collapse analysis showed a pure mode one collapse, with one half-wave shape passing through the mast length up to material failure and progressive deletion of the failed elements. Results are reported in terms of displacements (at mast head) versus reaction in Z direction at mast step, representing the corresponding compressive load (
) of the mast panel.

Figure 6. Collapse history: vertical displacements [mm] vs. vertical reaction [kN]

It can be noted that, after an initial linear elastic behaviour, a buckling load equal to 154 kN is clearly identifiable, corresponding to a vertical displacement of 15.4 mm. Then, the structure undergoes critical global buckling with decreasing reactive force, typical of cylindrical structures as well established in literature (e.g. Shama, 2013). It is also worth noting that a wide portion of the post-buckling response lies within the material elastic range, thus the post-buckling transition is fully reversible until local material failure, which takes place, actually, very near to the global collapse of the column, found at 138 kN with a corresponding mast head displacement of 67.5 mm. The large amount of elastic energy that the structure is capable to absorb in the post buckling stage is the main reason suggesting a dynamic analysis in time domain, to account for temporary non-equilibrated configurations capable of storing the work spent by the external forces for a limited amount of time.

5 DYNAMIC ANALYSIS

The dynamic load adopted in the present study is defined by a sinusoidal law where only half period is considered. The impulse is therefore defined by a period and an amplitude.
When the impulse drops to null value, it is kept constant to assess the subsequent structural response. The justification of the simplicity of such load function was due to the motivation of investigating the influence of inertial effects on the structural response. Therefore, there was no interest in simulating actual time history of loads at this stage of the study. The wave amplitude is defined by applying a scaling factor with respect to the critical load derived from the previously described progressive static collapse analysis. From an amplitude equal to the critical load found in the static analysis, the load is increased progressively up to obtain structural collapse, as shown in**Errore. L'origine riferimento non è stata trovata.**. Thirteen different periods have been considered, ranging from 0.05 s to 100 s, thus considering fast dynamic loads up to very long lasting ones, similar to a quasi-static case.

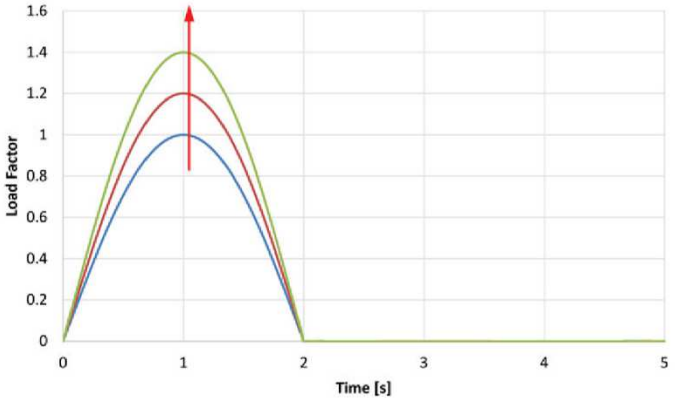

Figure 7. Dynamic loading function

As previously mentioned, the applied load is transferred from the load application point on the centre of the column head to the mast top end by means of a set of rigid links, as shown in Figure 4. The concentrated mass simulating the upper panels of the mast is placed on the same node where the force is applied. The con-

centrated mass should not be modelled as a force otherwise inertial contributions in terms of translations would be lost.
At the beginning of the computation, even with limited compressive impulse, a small vertical oscillation was observed in the model due to the effect of the concentrated mass, as in the initial configuration the non-deformed structure has to sustain the inertial force. Therefore, a suitably small value of damping was introduced in the computation to sweep away these physical oscillations due to the initial conditions. Damping was simulated according to the Rayleigh's approach, where the damping matrix **C** is considered as a linear combination of mass **M** and stiffness **K** matrices, each one multiplied by two different scalar coefficients, respectively named α and β (Equation 2).

$$\boldsymbol{C} = \alpha \boldsymbol{M} + \beta \boldsymbol{K} \qquad (2)$$

A sensitivity analysis was carried out on coefficients α and, β to achieve a critically damped system on the axial oscillation. Depending on the amplitude of the impulse, different behaviours of the mast panel have been identified as it follows.
The stable phase up to the buckling transition, where the rise of bending stresses in the mast is due to the rapid deformation, as the axial displacements (z direction) follow the loading time function and become null at a certain point in time. The transition point is coincident to the peak value of the load function for quasi-static loading conditions.
At higher loading rates, a particular point in time may be identified, where an unexpected behaviour is noted: while the applied load is being reduced according to the prescribed loading function, a growth in the axial displacement is found, followed by an oscillating behaviour. This fact is due to inertial effects, which delay the buckling effects. Thereafter, material failure of a few elements of the mast may or may not occur due to large deformations related to elastic buckling. However, the structure is able to restore its initial configuration with negligible damages, after the loading impulse is removed.
The mast collapse describes the condition where the mast panel is severely damaged so that it is no longer able to sustain its own weight due to several local failures of the material after complete removal of the applied load.

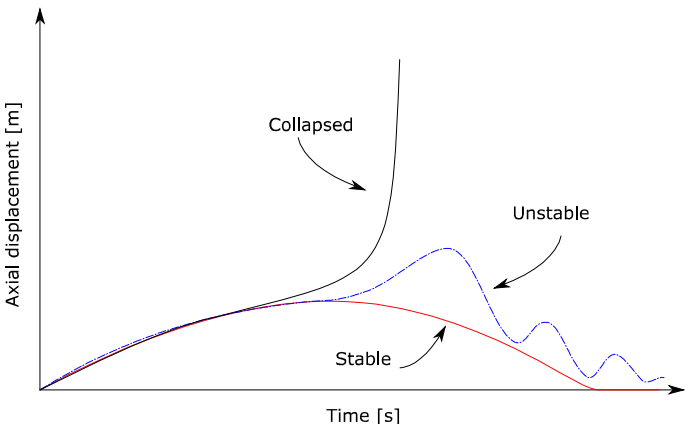

Figure 8. Time vs. axial displacement. Stable, unstable and collapsed behavior

Errore. L'origine riferimento non è stata trovata. shows an example of different solution trends in time, in terms of axial displacement of mast panel's top. It should be noted that the oscillations of the unstable transition curve may lead to either plastic or elastic strains, but the panel is still able to restore its initial configuration as long as no or limited laminate failure occurred.
As an example of an unstable behaviour, Figure 9 reports a local failure flag of the external ply of the CFRP laminate, for the case with load period of 2 seconds and load factor of 1.11.

Figure 9. Plies local failure. Load period 2 s, load factor of 1.11

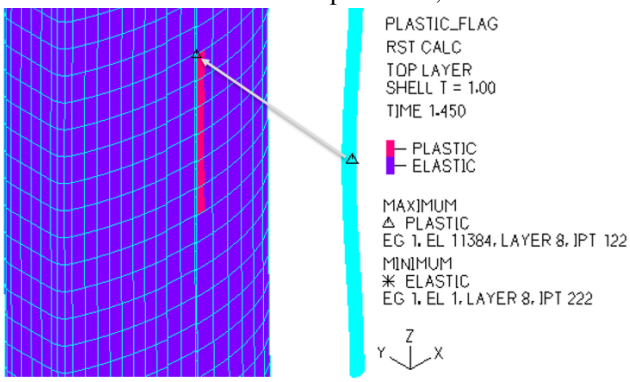

However, the mast was able to recover its original shape at the end of the calculation. On the other hand, this local failure will affect the structural strength and stiffness of the column, possibly resulting in a different structural response under further load cycles.
By the way, in the present study only one load cycle was considered, postponing further consideration on the effects of cyclical loads on ultimate collapse to future works. Local material failures have been detected at column's mid span for impulses having a period in a range of approximately 4 – 0.4 seconds. Below this threshold, failure was mainly localized close to the bottom-constrained zone.

6 DISCUSSION OF RESULTS

As mentioned, in the present study thirteen different impulse time durations have been considered ranging from 0.05 s to 100 s. For each impulse duration, conditions of global collapse, local rupture and instability are reported along with the corresponding load factor amplitude (Figure 6). It can be noted that for load impulses equal or longer than 10 s, i.e. 0.1 Hz period, no local failures occur but the mast panel directly switches from a local unstable configuration to the global collapse, as typically experienced by slender columns whose collapse is driven by elastic buckling

(Euler's buckling). On the other hand, for load duration shorter than 0.2 s, i.e. 2.5Hz, buckling does not occur.

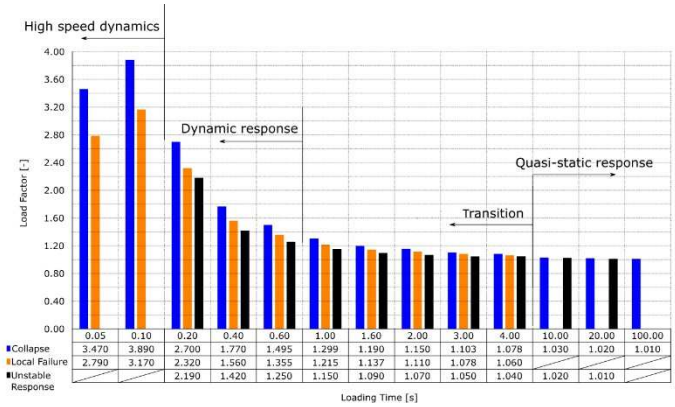

	0.05	0.10	0.20	0.40	0.60	1.00	1.60	2.00	3.00	4.00	10.00	20.00	100.00
Collapse	3.470	3.890	2.700	1.770	1.495	1.299	1.190	1.150	1.103	1.078	1.030	1.020	1.010
Local Failure	2.790	3.170	2.320	1.560	1.355	1.215	1.137	1.110	1.078	1.060			
Unstable Response			2.190	1.420	1.250	1.150	1.090	1.070	1.050	1.040	1.020	1.010	

Figure 6. Load time vs. load factor, different structural responses

Four different regions can be observed depending on the load application time:
A quasi-static response region, from 10 s to 100 s, where the dynamic effects are negligible and the collapse behaviour replicates the static model.
A transition zone, from 4.0 s to 1.0 s, where an increment of the sustainable load is noted when reducing the application period of the load.
A dynamic response region, from 0.6 s to 0.2 s, where significant increment in the sustainable load is found, as the structure becomes very sensitive to variations of the impulse duration.
A high-speed dynamics range, below 0.2 s, where local ruptures directly lead to global collapse following a progressive path.
It is worth noting that the transition zone and the dynamic region are characterized by load application periods approximately corresponding to those of the wave encounter frequency typical of large sail ships. Moreover, induced ship motions as well as wind load on the sail system are characterized by relatively shorter periods and vibration induced loads stress the mast panels when motoring and in rough sea. As a matter of facts, large sail ships are rather stiff ships in sea waves because of keel weight and stability needs. Further considerations about these different zones will be hereunder presented in more detail.

6.1 *Quasi-static region*

In this region, the mast works like a typical compressed slender column: dynamics effects have very little or no importance and the presence of a compressive force even slightly higher than the static critical load leads to collapse due to global buckling. In fact, the global collapse, the local failure and the elastic buckling are almost coincident in terms of axial applied force. Hence, once the elastic buckling load is reached, the column fails to sustain any higher load and it behaves like an Euler column (i.e. a purely global instability is observed in practice, with no residual capacity). The definition of the limit of such zone could be a useful parameter for the rig designer, avoiding dynamic time-consuming computations since static models are adequate to predict the collapse. Of course, further deepening should be carried out to assess different mast geometries and dimensions obtain a general rule requirement useful in engineering design practice but the trend is quite clear.

6.2 *Transition zone*

In this zone, the critical load is slightly influenced by the duration of the load, i.e. the smaller the duration of the applied load, the higher the mast response. Differences among estimated collapse loads are more evident, as the load impulse becomes faster (shorter period of application).
Three distinct load thresholds become clearly visible:

- Elastic buckling with elastic material response,
- Material failure of local elements not affecting the global capacity, with the mast resuming its original configuration after the load is removed,
- Global collapse of the mast.

6.3 *Dynamic region*

This zone revealed to be very critical. In fact, even slightly varying load duration induces considerable differences in maximum sustainable load. The structure is able to withstand collapse loads from 1.8 to 2.7 times higher with respect to the statically applied load, depending on the impulse period. Moreover, a higher gap between the buckling limit and the local rupture one is observed, indicating a remaining margin between the elastic buckling and the initiation of the mast collapse.

6.4 *High-speed dynamics range*

In this region, an increase of the maximum sustainable load is observed until periods of about 0.1 s, whilst a drop is observed at 0.05 s. The study was not deepened for higher load frequencies since phenomena of such small duration are not likely to occur on sail systems but it should be noted that such a limit depends on the features of the structure. It should be also noted that in this region no elastic buckling is observed, differently to what reported by Gaiotti and Rizzo (2014) where the aluminium mast showed a failure mode clearly driven by local buckling phenomena.
In the present case, above a certain load amplitude, material failure at the bottom of the mast occurs, quickly leading to global collapse. In order to better understand the physics behind fast growing external forces, for the case of loads acting for 0.05 s, a graph reporting vertical displacements at mast panel's top and the loading time function (scaled) over time is reported in Figure 11.

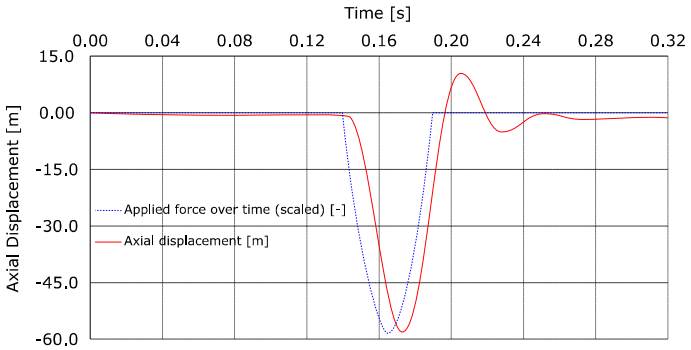

Figure 7. Axial displacement delay for load of 0.05 s duration.

A delay between the load and the vertical displacements can be observed because of inertial effects. A positive extensional displacement was detected after the applied force had ceased. This fact means that the strain energy does not balance the external work in the unloading phase leading to a much higher amount of energy to be stored in the system, both in form of strain energy and kinetic energy.
Therefore, when the load is removed, the column behaves similarly to an oscillating one Degree of Freedom (1-DoF) dynamic system.
However, to better understand the collapse mechanism, a new plot reporting the reaction force at the constrained mast end versus the applied force at the mast top is reported (**Errore. L'origine riferimento non è stata trovata.**).

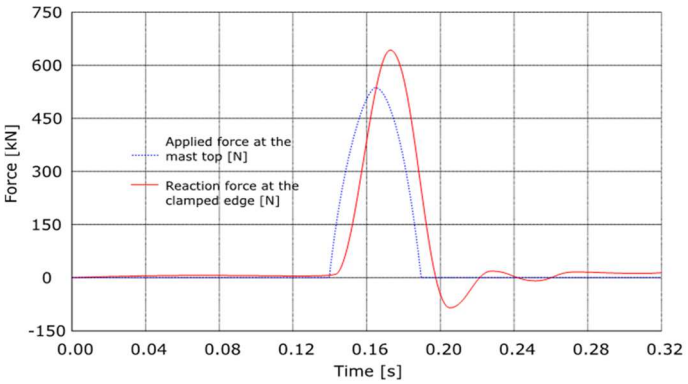

Figure 8. Reaction force delay for load of 0.05 s duration.

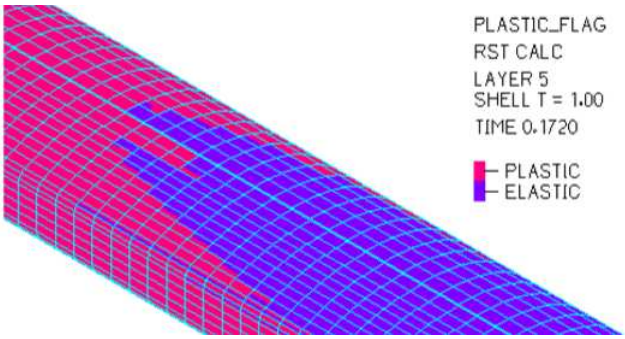

Figure 13. Large failure zone nearby the clamped edge

Besides the delay between the two curves, it can be noted that value of the reaction is higher than the applied force, due to the previously mentioned energetic consideration. This is mainly due to inertial effects, i.e. to the fact that the kinetic energy leads to a normal compressive wave, which induces an increased compression located at the clamped end.
Figure 13 reports a large zone where elements experience material failure nearby the clamped edge.

7 COMPARISON WITH ALUMINIUM MAST

In this section, a comparison between the CFRP mast analysed in the present work and an analogous one built in aluminium alloy and studied in a previous work (Gaiotti and Rizzo, 2014), is presented. Figure 14 shows the masts' cross section for both models.

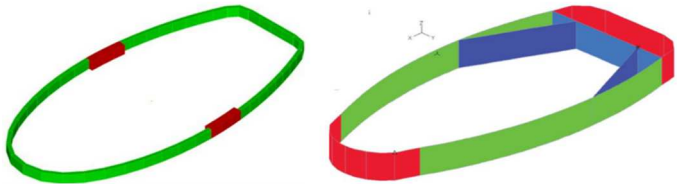
Figure 14. Cross-sections of composite mast (left) and aluminium mast (right)

The section of the aluminium mast is 900 mm long and 400 mm wide, the mast tube thickness ranges from 8 to 12 mm, while the internal frames are 5 mm (main) and 4 mm (lateral) thick. The mast section was used for similar sail ships, approximately of the same size, whose sail system was different mainly because of the building material of the mast. Indeed, the same shipyard built and launched various similar hulls having different mast and rigging designs. However, the same mast panel length was considered (10 m) and the same concentrated mass simulating the upper part of the mast was applied at the top (5000 kg) for comparison purposes.
Figure 15. Comparison between carbon and aluminium masts.

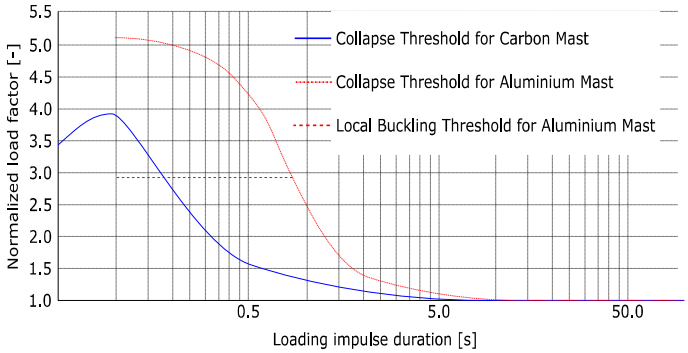

Despite dimensions are different as well as column stiffness (and so numerical results), a similar trend between collapse curves can be observed in Figure 15, showing that these slender structure can withstand loads considerably higher if loads are applied only for short periods of time rather than statically or as long-lasting forces. Further comparisons will be carried out in the future among different masts geometries. Eventually, it should be noted that, in case of aluminium masts, a threshold indicating the initiation of local instabilities (i.e. local buckling) was highlighted for

high-speed dynamics loads, whilst for the carbon mast no local buckling occurred. Moreover, the aluminium mast seems to be more sensitive to dynamic effects, likely due to the different mass/stiffness ratio with respect to CFRP.

8 CONCLUSIONS

In this paper, a numerical investigation on the dynamic buckling behaviour of a typical CFRP mast panel employed in sailing yacht industry has been carried out assessing the dependency of the mast's response with respect to impulsive loads applied for different periods. This work followed a previous one regarding aluminium masts (Gaiotti and Rizzo, 2014).
Present results confirmed that the mast is able to resist to higher loads for relatively high load application rates, indicating an inverse proportionality between the maximum sustainable load and the load impulse duration. However, localized failures may occur, affecting structural behaviour in forthcoming load cycles. A simplified sinusoidal load function was adopted in this study to assess the inertial effects and their involvement into the elastic buckling problem of a column, whose main outcomes are the following:
The structure showed a growing ultimate strength level when reducing the acting period of the load.
The instability condition has been reached with a delay with respect to the maximum applied load, while the stress level was actually decreasing. This is mainly caused by inertial effects, but it is also due to the delay in displacement of the mast top, leading to axial displacements in the direction of the applied force also after the load peak has been reached, leading to a positive work of the external force. Furthermore, it should be remembered that collapse could be due to an excessive stress level as well as a variation in the stiffness of the structure due to large displacements experienced because of the buckling.
Therefore, results confirmed the general trend observed on aluminium masts, highlighting only minor conceptual differences. Actually, local buckling does not occur in carbon masts in the high-speed dynamics region. Further comparison will be carried out in the future, comparing masts of different material and geometries.
In conclusion, the present work showed interesting results on the capability of column-like structures to withstand dynamic loads, i.e. loads acting for a short period of time, having a significant higher magnitude than static loads. In order to extend the study and determining new possible guidelines in the design of mast and rigging structures, different mast panel features (e.g. span, cross section geometries, stacking sequences), more complex loading conditions as well as the modelling of the whole rig including manufacturing defects could be taken into account in future studies.

9 REFERENCES

ADINA, 2016. Theory and Modeling Guide v.9.2. ADINA R&D. Watertown, MA, USA

Augier B., Bot P., Hauville F., Durand M., 2013. Dynamic behaviour of a flexible yacht sail plan. Ocean Engineering 66,32-43

Bathe K.J., 1996. Finite Element Procedures, Prentice Hall. Upper Saddle River, USA

Chapelle D., Bathe K.J., 2011. The finite element analysis of shells - Fundamentals. Springer, Berlin Heidelberg

DNVGL, 2016. Design and construction of large modern yacht rigs (DNVGL-ST-0412), DNVGL AS, Hamburg, 2016

Fossati F., Muggiasca S., 2011. Experimental investigation of sail aerodynamic behavior in dynamic conditions, SNAME 2012 Annual Meeting and Expo and Ship Production Symposium, Providence, USA, J Sailboat Technology, Article 2011-02

Gaiotti M., Rizzo C.M., 2014. Dynamic buckling of masts of large sail ships. Ships Offshore Structures 10(3),290-301

Lepidi M., Ghelardi S., Rizzo C.M., 2015. A nonlinear monodimensional beam model for the dynamic analysis of the mast pumping phenomenon in sailing boats. 22nd AIMETA Conference, 14-17 September 2015 Genoa, Italy

Lorenzetti, A., Gaiotti, M., Ghelardi, S. & Rizzo, C., 2017. Reduced Finite Element Models for Mast Analysis. MARSTRUCT, 6th International Conference on Marine Structures, Lisbon, Portugal.

Menotti, W., Durand, M., Gross, D., Roux, Y., Glehen, D., Dorez, L., 2013. An Unsteady FSI Investigation Into The Cause Of The Dismasting Of The Volvo 70 Groupama 4. 26th - 28th June, Innov'Sail Lorient, France.

Raftoyiannis J., Spyrakos C., 1997. Linear and nonlinear FE analysis in engineering practice. Algor Inc. Publishing Division, Pittsburgh

Rizzo C.M., Carrera G., Paci M., 2009. Structural monitoring of mast and rigging of sail ships, In: Das P., Guedes Soares C. (Eds.) Analysis and design of marine structures. CRC Press, Boca Raton, pp. 333-343

Rizzo C.M., Boote D., 2010. Scantling of mast and rigging of sail boats: a few hints from a test case to develop improved design procedures, Proc.s 11th Int Symp Pract Des Ships & Float Struct PRADS 2010, COPPE, Rio de Janeiro, Brasil, 20–24 September 2010, pp. 613-623

Sacher M., Hauville F., Bot P., Durand M., 2015. Sail Trimming FSI Simulation - Comparison of Viscous and Inviscid Flow Models to Optimise Upwind Sails Trim, Proc. 5th High Performance Yacht Design Conf HPYD2015, Auckland, New Zealand, 10-12 March 2015, pp. 217-228

Shama M., 2013. Buckling of Ship Structures. Springer-Verlag, Berlin Heidelberg

Shenoi A., Beck R., Boote D., Davies P., Hage A., Hudson D., Kageyama K., Keuning J.A., Miller P., Sutherland L., 2009. Report of Specialist committee V.8 on sailing yacht design. Proc. 17th Int Ship Offshore Struct Congr, Seoul, Korea, 16-21 August 2009

Skene N., 1938. Elements of yacht design. 1938, as published by Sheridan House Inc., New York, 2001

Trimarchi D., Rizzo C.M., 2009. A FEM-Matlab code for fluid structure interaction coupling with application to sail aerodynamics of yachts, Proc. 13th Int Congr Int. Marit Association Mediterranean IMAM 2009, Istanbul, Turkey, 12–15 October 2009, pp. 907-916

Viola I., Bartesaghi S., Van-Renterghem T., Ponzini R., 2014. Detached Eddy Simulation of a Sailing Yacht, Ocean Eng 90,93-103